Participation of the Disulfide Bridge in the Redox Cycle of the Ferredoxin from the Hyperthermophile *Pyrococcus furiosus*: ^{1}H Nuclear Magnetic Resonance Time Resolution of the Four Redox States at Ambient Temperature†

Carol M. Gorst,‡ Zhi Hao Zhou,§ Kesen Ma,§ Quincy Teng,‡ James B. Howard,|| Michael W. W. Adams,*,§ and Gerd N. La Mar‡

Department of Chemistry, University of California—Davis, Davis, California 95616, Department of Biochemistry and Molecular Biology, University of Georgia, Athens, Georgia 30602, and Department of Biochemistry, University of Minnesota, Minneapolis, Minnesota 55455

Received February 17, 1995; Revised Manuscript Received April 18, 1995⊗

ABSTRACT: The oxidized and reduced forms of the [4Fe−4S]-containing ferredoxin from the hyperthermophilic archaeon *Pyrococcus furiosus*, *Pf*, have been investigated by ^{1}H nuclear magnetic resonance spectroscopy, electron paramagnetic resonance spectroscopy and thiol titrations. We have identified and isolated at ambient temperature four distinct redox states for the [4Fe−4S] form of the ferredoxin. These states differ in the redox state of the cluster, which is coordinated by Cys 11, Asp 14, Cys 17, and Cys 56, and of a disulfide bridge between Cys 21 and Cys 48. The protein, as isolated under anaerobic conditions, designated 4Fe Fd_B^{red}, contains the reduced cluster and two free thiols. The cluster, but not the thiols, is readily oxidized by brief exposure to O_2 to yield 4Fe Fd_B^{ox}. Prolonged O_2 treatment (>24 h at 30 °C) is required to generate the protein with a disulfide (4Fe Fd_A^{ox}) while this fully oxidized form is readily converted by brief reduction with sodium dithionite to the protein with a reduced cluster and a disulfide (4Fe Fd_A^{red}). Analyses of the magnitude and the number of hyperfine-shifted resonances in each of the four redox states are discussed.

Ferredoxin, Fds,[1] are small (56−66 residues) electron transfer proteins that possess one or more iron−sulfur clusters as the redox active chromophore. They are generally classified into the plant-type or two-iron Fd, which exist in the oxidation states $[Fe_2S_2]^{1+,2+}$, and the bacterial-type or cubane four-iron Fds, where the oxidation states are $[Fe_4S_4]^{1+,2+}$. In some Fds the latter cubane-type cluster can also be present in a modified form as a three-iron cluster $[Fe_3S_4]^{0,1+}$. Bacterial-type Fds can possess either one or two clusters and 3Fe, 4Fe, 7Fe, and 8Fe Fds are known, with each cluster capable of serving as a one-electron carrier but not necessarily at a similar potential. The binding of the cluster (designated as cluster 1) that is common to both one- and two-cluster Fds occurs via the consensus sequence Cys^{I}-X-X-Cys^{II}-X-X-Cys^{III}-$(X)_nCys^{IV}$, where Cys^{I-III} reside near the N-terminus and Cys^{IV} is close to the C-terminus (Cammack et al., 1977; Beinert, 1990). A schematic example is shown in Figure 1. The two-cluster Fds possess an additional four Cys for the second cluster (designated cluster 2) for which the pattern of Cys spacing is the same, with three of the ligands near the C-terminus. The crystal structures of two 8Fe Fds are known, those of *Peptococcus aerogenes*, *Pa* (Adman et al., 1976), and *Clostridium acidurici* (Duee et al., 1994), and the consensus-sequence symmetry manifests itself in pseudo-2-fold structural symmetry for the both molecules.

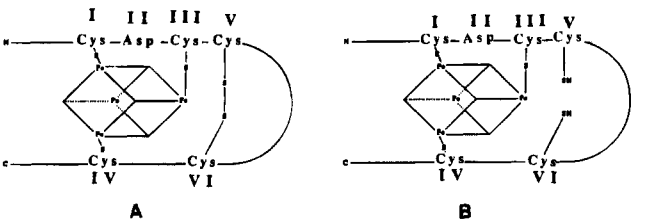

FIGURE 1: Schematic representation of the consensus sequence for the ligating Cys I−IV for cluster 1 in a bacterial 4Fe Fd. Two of the four Cys for the consensus sequence for cluster 2 have been deleted. The two retained Cys from cluster 2, Cys V and Cys VI, can form a disulfide bridge (A) or remain as free Cys (B). Cys II is not ligated in *Dg* 3Fe Fd, and Cys II is replaced by Asp in *Pf* Fd and is likewise not ligated in the 3Fe form.

The single-cluster Fds have been proposed to evolve from the two-cluster proteins by the mutation of two or more of the Cys in the consensus sequence for cluster 2 (Beinert, 1990). The prototypical examples, both of which have been crystallographically characterized, are the 4Fe Fd from *Bacillus thermoproteolyticus*, *Bt*, for which all four Cys for cluster 2 have been replaced (Fukuyama et al., 1988), and the 3Fe Fd from *Desulfovibrio gigas*, *Dg*, which lacks two Cys of the consensus sequence in cluster 2 (Kissinger et al., 1991). In these proteins, an α-helix was found in the

† This research was supported by grants from the National Science Foundation, DMB-90-04018 (G.N.L.), MCB 94-05783 (M.W.W.A.), DMB-91-20515 (J.B.H.), and the National Institutes of Health, GM 45597 (M.W.W.A.).

* Address correspondence to this author at the Department of Biochemistry, Life Sciences Bldg., University of Georgia, Athens, GA 30602-7229.

‡ University of California—Davis.

§ University of Georgia.

|| University of Minnesota.

⊗ Abstract published in *Advance ACS Abstracts,* June 15, 1995.

[1] Abbreviations used: NMR, nuclear magnetic resonance; 2D, two dimensional; DSS, 2,2′-dimethyl-2-silapentane-5-sulfonate; Fd, ferredoxin; HiPiP, high-potential iron−sulfur protein; TOCSY, total correlation spectroscopy; NOESY, nuclear Overhauser spectroscopy; WEFT, water-eliminated Fourier transform; *Pf*, *Pyrococcus furiosus*; *Dg*, *Desulfovibrio gigas*; *Pa*, *Peptococcus aerogenes*; *Bt*, *Bacillus thermoproteolyticus*; POR, pyruvate ferredoxin oxidoreductase; SuDH, sulfide dehydrogenase; EPR, electron paramagnetic resonance; DTNB, 5,5′-dithiobis(2-nitrobenzoic acid).

0006-2960/95/0434-8788$09.00/0

environment of the deleted cluster 2, and it has been proposed that such an α-helix will be present in all one-cluster bacterial Fds (Fukuyama et al., 1988). Solution ^{1}H NMR studies of several such one-cluster Fds support this hypothesis (Marion & Guerlesquin, 1989; Teng et al., 1994). In the *Dg* protein, the two Cys that remain from the consensus sequence for cluster 2 form a disulfide bridge (*i.e.*, Figure 1A), as revealed in the crystal structure of the oxidized 3Fe form of this protein (Kissinger et al., 1991). This observation was first viewed with skepticism since disulfide bridges are rarely found in intracellular proteins. This disulfide bridge, therefore, represents an alternate or additional site capable of electron transfer and must be considered in understanding the redox cycle of single-cluster Fds.

The single-cluster Fd from the hyperthermophilic archaeon *Pyrococcus furiosus*, *Pf* (optimal growth at temperatures near 100 °C), is purified in its functional 4Fe form, but in contrast to most other Fds, it is readily converted to the 3Fe form *in vitro* (Conover et al., 1990; Park et al., 1991). Pf Fd is remarkably thermostable in both its 3Fe and 4Fe form (it can be incubated anaerobically for 24 h at 95 °C without detectable denaturation) and exhibits significant sequence homology (34% identity) to *Dg* Fd (Busse et al., 1992). The facile interconversion of the two cluster forms in *Pf* Fd may be related to the substitution of one Cys (Cys^{II} replaced by Asp 14) in the cluster-binding consensus sequence. Two remaining Cys (V and VI in Figures 1 and 2) present in *Pf* Fd are homologous to those participating in the disulfide bridge in *Dg* Fd. The initial results of a solution NMR structure determination of the secondary structure for *Pf* 3Fe Fd^{ox} revealed a folding topology similar to that of *Dg* 3Fe Fd^{ox} but with significant extension of several secondary structural motifs (Teng et al., 1994). These include the incorporation of a third strand into the β-sheet involving the terminus and a lengthening and translation to bring the N-terminus nearer to the major α-helix. Backbone NOEs for residues near Cys^{21} and Cys^{48} indicated that Cys^{V} and Cys^{VI} participate in a disulfide bridge in oxidized *Pf* 3Fe Fd.

We present herein ^{1}H NMR data on the electronic/molecular structure of the 4Fe form of *Pf* Fd which demonstrate that the cycle between the reduced and oxidized forms of the protein encompasses four distinct states of the molecule involving independently the cluster and the disulfide bridge. The basis for distinguishing these states rests with the characteristic hyperfine shift pattern and its temperature dependence, features that are exhibited by the ligated Cys C_βHs in a wide variety of characterized cubane-type iron−sulfur cluster proteins (Phillips & Poe, 1973; Bertini et al., 1991, 1992; Luchinat & Ciurli, 1993; Donaire et al., 1994), together with thiol titrations of the protein. The participation of a disulfide group in the redox cycle had no published precedent for an iron−sulfur cluster protein prior to 1994. However, while this work was in progress, a similar conclusion was reached for *Dg* 3Fe Fd, in which reduction of the disulfide-containing oxidized protein was shown to require three electrons, one for the cluster and two for the disulfide (Macedo et al., 1994). We show here that the 4Fe form of *Pf* Fd can be prepared in four distinct and stable redox states at ambient temperature, and the same appears to be also true for the 3Fe Fd.

MATERIALS AND METHODS

Pyrococcus furiosus (DSM 3638) was grown in a 600-L fermenter and its ferredoxin was purified under strictly anaerobic conditions in the presence of sodium dithionite as described previously (Aono et al., 1989). The pure protein was stored frozen as pellets in liquid N_2 and was thawed when required. Where indicated, sodium dithionite was removed from samples by gel filtration (Superdex G-50) in a vacuum atmosphere glove box. When samples were reduced with excess sodium dithionite, the pH was adjusted after the addition. Samples for NMR spectroscopy were equilibrated with 50 mM sodium phosphate buffer, pH 7.6, or with 50 mM Tris buffer, pH 8. Where indicated, samples were exchanged into 95% ^2H_2O/5% ^1H_2O in an Amicon ultrafiltration device utilizing a YM 3 membrane.

Pyruvate ferredoxin oxidoreductase (POR) (Smith et al., 1994), sulfide dehydrogenase (SuDH) (Ma & Adams, 1994), and hydrogenase (Bryant & Adams, 1989) were purified from *Pf* as previously described. The Fd-dependent activity of a reconstituted system comprised of POR, SuDH, and hydrogenase (Ma et al., 1994) were measured as indicated. *Pf* Fd was converted from its native 4Fe form to the 3Fe form by the addition of potassium ferricyanide at pH 7.6 (Conover et al., 1990). Limiting amounts of ferricyanide were added under anaerobic conditions for partial conversion of 4Fe Fd_B^{ox} protein to 3Fe Fd_B^{ox} conformation (see below). Complete conversion under anaerobic conditions was achieved by addition of an excess of ferricyanide. Incubation of 4Fe protein with excess ferricyanide under aerobic conditions, or incubation of 3Fe Fd_B^{ox} protein with O_2, was used to generate 3Fe Fd_A^{ox}. Samples were prepared for monitoring the effect of oxidant concentration on conversion of 4Fe Fd_B^{ox} to 4Fe Fd_A^{ox} by exposing the as-isolated protein to air and splitting the sample into two aliquots. The first aliquot was monitored directly, and the second aliquot was degassed with successive cycles of vacuum/Ar flushing to remove O_2. After 30 days the second aliquot was gassed for 1 min with pure O_2 and the conversion to 4Fe Fd_A^{ox} was monitored to completion.

The thiol content of the various protein preparations was determined spectrophotometrically by their reaction with 5,5′-dithiobis(2-nitrobenzoic acid) (DTNB) as described by Riddles et al. (1983). *Pf* 4Fe Fd_B^{red} was separated from sodium dithionite (which reacts with DTNB) by gel filtration and was collected under Ar. The protein was transferred to anaerobic, septum-sealed cuvettes containing 0.1 M sodium phosphate, pH 7.1 (1.0 mL final volume). After the spectrum of the protein was recorded, the absorbance at 412 nm was monitored for 2−5 min before the addition of DTNB (0.2 mM final concentration). Three other redox states of the protein were prepared (see Results for origin of nomenclature). 4Fe Fd_B^{ox} was prepared by treating 4Fe Fd_B^{red} with O_2 for 15 min followed by deoxygenation and purging with Ar. 4Fe Fd_A^{ox} was prepared by treating 4Fe Fd_B^{red} with O_2 for 36 h at 30 °C followed by deoxygenation. 4Fe Fd_A^{red} was prepared by treating 4Fe Fd_A^{ox} with 5-fold excess sodium dithionite for 15 min at 30 °C followed by anaerobic gel filtration. The DTNB reaction was monitored at 30 °C for 12 h. At the end of the 30 °C incubation, the temperature was raised to 80 °C and the monitoring was continued. Prior to thiol analysis, samples were injected into Ar-flushed EPR tubes and rapidly frozen in a liquid N_2−heptane mixture.

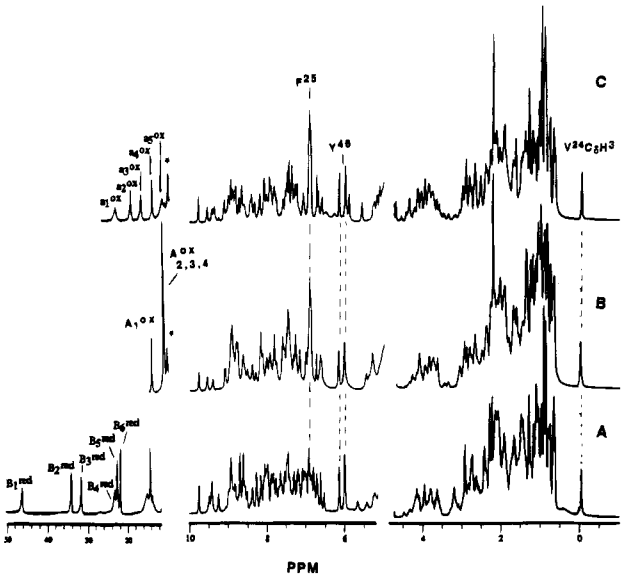

FIGURE 2: Complete 500-MHz ^1H NMR spectra under nonsaturating conditions (0.33 scan/s) in ^1H_2O, pH 8.0, at 30 °C of (A) as-isolated, reduced *Pf* 4Fe Fd, designated *Pf* 4Fe Fd_B^{red}, with contact-shifted nonlabile proton peaks B_i^{red}, (B) the terminally oxidized form, designated *Pf* 4Fe Fd_A^{ox}, with contact-shifted nonlabile proton peaks, A_i^{ox}, and (C) the previously characterized terminally oxidized form of *Pf* 3Fe Fd (Busse et al., 1993), here designated *Pf* 3Fe Fd_A^{ox}, with nonlabile proton peaks a_i^{ox}. All NMR samples were ~8 mM. Labile proton peaks are labeled by asterisks. The regions 50−10 ppm and 10−5 ppm are expanded vertically by factors of 3 and 2, respectively, when compared with the 5−0 ppm window.

EPR spectra were recorded at 10 K on an IBM−Bruker ER200D spectrometer interfaced to an IBM 9001 microcomputer and equipped with an Oxford Instruments ESR-9 flow cryostat. ^1H NMR spectra were recorded at 500 MHz on a GE Omega 500 spectrometer and at 300 MHz on a GE Omega 300 spectrometer. Chemical shift values were referenced to 2,2-dimethyl-2-silapentane-5-sulfonate, DSS, through the residual solvent signal. One-dimensional spectra were collected by the normal one pulse with ^1H_2O presaturation or the super-WEFT (Inubishi & Becker, 1983) pulse sequence over a range of recycle times (80−500 ms). T_1 data were collected with a standard inversion recovery pulse sequence and the T_1 values were approximated from the null point. 2D ^1H NMR experiments were performed at 500 MHz. Data were collected at 30 °C over a 7017-Hz sweep width and consisted of 96 transients collected over 2048 complex points and over 512 t_1 increments. For 2D TOCSY experiments an MLEV 17 spin-lock was applied for 50 ms. NOESY spectra were recorded with 250-ms mixing times. Data were processed as described in Teng et al. (1994). All samples were in 50 mM phosphate, pH 7.6, in H_2O and ranged in concentration from 5 to 8 mM.

RESULTS

Protein Folding. The complete 500-MHz ^1H NMR trace in ^1H_2O of the anaerobically isolated (dithionite-reduced) *Pf* 4Fe Fd (which we designate 4Fe Fd_B^{red}, where the superscript refers to the cluster oxidation state; see below), is illustrated in Figure 2A, and that of the final product of oxidation in the presence of excess O_2 (designated 4Fe Fd_A^{ox}; see below) is shown in Figure 2B. Each spectrum may be compared with that of the previously characterized oxidized *Pf* 3Fe Fd (designated 3Fe Fd_A^{ox}; see below) in Figure 2C. In all cases, the spectra represent the equilibrium species under conditions of "excess reductant" (Figure 2A) or "excess oxidant" (Figure 2B,C) (see below).

Table 1: ^1H NMR Chemical Shift Data for Selected Noncoordinated Residues of *Pf* Fd[a]

residue	position	4Fe Fd_B^{red}	4Fe Fd_B^{ox}	4Fe Fd_A^{ox}	4Fe Fd_A^{red}	3Fe Fd_A^{ox}
Trp^2	7H	6.93	6.95	6.89		6.86
	6H	6.85	6.86	6.89		6.89
	5H	6.53	6.52	6.61	6.52	6.57
	4H	7.30	7.34	7.33	7.19	7.30
	2H	6.61	6.64	6.74	6.78	6.71
Phe^{25}	ring Hs	7.00	6.99	6.98	6.94	6.91
		6.79	6.73	6.89	6.84	
		6.72				
Val^{24}	NH	7.44		7.82		7.63
	$C_\alpha H$	3.91		3.89		3.91
	$C_\beta H$	1.50		1.56		1.43
	$C_{\gamma 2H3}$	−0.07	−0.02	0.00	−0.01	−0.05
	$C_{\gamma 1H3}$	0.59	0.64	0.85	0.80	0.76
Asn^{47}	NH	8.06	8.07	8.3		8.22
	$C_\alpha H$	3.82	3.80	3.84		3.83
	$C_\beta H$	2.65	2.71	2.70		2.68
	$C_{\beta H'}$	2.76	2.84	2.80		2.79
	$N_{\delta H}$	7.14	7.10	6.92		6.94
	$N_{\delta H'}$	7.80	7.50	7.40		7.44
Tyr^{46}	NH	7.97	8.01	7.77		7.76
	$C_\alpha H$	3.65	3.68	3.65		3.65
	$C_\beta H$	2.41	2.46	2.42		2.42
	$C_{\beta H'}$	2.04	2.09	2.06		2.00
	$C_{\delta Hs}$	5.99	6.01	6.01	6.04	6.02
	$C_{\epsilon Hs}$	6.12	6.15	6.16	6.19	6.17

[a] Chemical shifts were taken from NOESY data (except for 4Fe Fd_A^{red}, for which the chemical shifts for resolved peaks were obtained from a standard 1D spectrum), collected at 30 °C for samples in ^1H_2O, pH 8.0; data for 3Fe Fd_A^{ox} were taken from Teng et al. (1994).

The diamagnetic envelopes, 0−10 ppm, for the three *Pf* Fd forms in Figure 2 have a similar pattern of shifts, which reflects a folding topology similar, but not identical, to that reported in detail for *Pf* 3Fe Fd_A^{ox} (Teng et al., 1994). Preliminary 2D NMR data identify the major contacts involving the aromatic side chains. Scalar correlation (TOCSY) data (not shown) identify the side-chain signals for three aromatic side chains, Trp^2, Phe^{25}, and Tyr^{46}, as well as that of a strongly ring-current-shifted Val^{24}. NOESY data confirm the strong interaction between Val^{24} and Phe^{25} and between Trp^2 and Tyr^{46} in both 4Fe Fd forms, as previously reported for the 3Fe Fd_A^{ox}. Two peptide NHs show NOESY cross peaks to the Tyr^{46} ring, and the combination of TOCSY and NOESY spectra identify them as those from Tyr^{46} and Asn^{47}, for which the complete residues are assigned. In each case, the Tyr^{46} and Asn^{47} NHs are part of an extended N_i−N_{i+1} NOESY pattern shown previously to arise from an α-helix in 3Fe Fd^{ox} (Teng *et al.*, 1994). The chemical shifts for these five residues are listed in Table 1.

Hyperfine-Shifted Signals. The resonances to the low field of ~10 ppm in Figure 2 arise from the hyperfine-shifted and relaxed $C_\beta H$ and/or $C_\alpha H$ of the ligated residues (Phillips & Poe, 1973), primarily Cys but also possibly Asp.[2] The anaerobically isolated 4Fe Fd^{red} exhibits numerous low-field resolved and strongly relaxed (T_1 ~ 2−30 ms) single proton

[2] Asp 14, substituted for Cys II in the cluster binding consensus sequence, is in proximity to ligate to the cluster. The number and pattern of hyperfine-shifted resonances in reduced 4Fe *Pf* Fd suggest this ligation occurs. Steady-state 1D NOE studies in combination with saturation transfer experiments between the oxidized and reduced protein and TOCSY experiments on oxidized 4Fe *Pf* Fd strongly suggest the Asp is ligated in both the oxidized and reduced forms of the protein (Gorst, unpublished results).

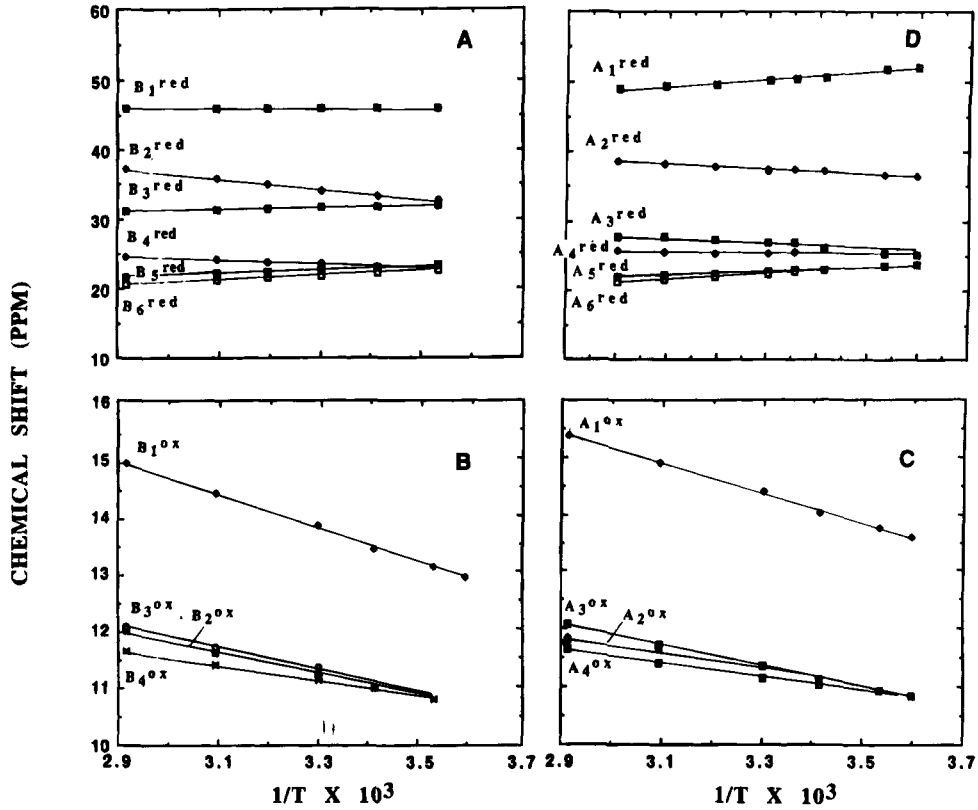

FIGURE 3: Plot of observed chemical shift at 30 °C, referenced to DSS, for well-resolved low-field contact-shifted ligand resonances versus reciprocal absolute temperature (Curie plot). (A) *Pf* 4Fe Fd_B^{red} with peaks B_i^{red}; (B) *Pf* 4Fe Fd_B^{ox} with peaks B_i^{ox}; (C) *Pf* 4Fe Fd_A^{ox} with peaks A_i^{ox}; (D) *Pf* 4Fe Fd_A^{red} with peaks A_i^{red}. Peaks with positive and negative slopes are designated Curie-like and anti-Curie, respectively.

resonances (labeled B_i^{red}) in Figure 2A in a spectral window typical of a Fd with a reduced $[Fe_4S_4]^{1+}$ cluster. The temperature dependence of the six well-resolved low-field peaks for 4Fe Fd_B^{red}, as shown in Figure 3A, is of both the Curie- and anti-Curie type. This behavior is characteristic of proteins with clusters containing one pair of valence-delocalized iron ($2Fe^{2.5+}$), such as found for $[Fe_4S_4]^{1+}$ in reduced Fd and for $[Fe_4S_4]^{3+}$ in oxidized high-potential iron–sulfur protein, HiPiP (Phillips & Poe, 1973; Bertini et al., 1991, 1992; Luchinat & Ciurli, 1993; Donaire et al., 1994).

Pf 4Fe Fd_A^{ox} exhibits four low-field relaxed resonances ($T_1 \sim 3-15$ ms), labeled A_i^{ox} in Figure 2B, all of which exhibit anti-Curie behavior as shown in Figure 3C. Such singular anti-Curie behavior is characteristic of the $S = 0$ ground state with thermal population of excited paramagnetic states of a $[Fe_4S_4]^{2+}$ cluster of either oxidized Fd or reduced HiPiP (Phillips & Poe, 1973; Banci et al., 1990; Luchinat & Ciurli, 1993; Donaire et al., 1994). Hence the ^1H NMR spectral characteristics in the hyperfine-shifted region of *Pf* 4Fe Fd_A^{ox} and 4Fe Fd_B^{red} exhibit the properties characteristic of the oxidized and reduced cluster states, respectively, of a typical 4Fe-type Fd. The chemical shift for the well-resolved hyperfine-shifted peaks to the low field of 10 ppm are listed in Table 2.

Redox Cycling of 4Fe Fd. The redox cycle of *Pf* Fd can be observed in the low-field region of the 500-MHz ^1H NMR spectra (Figure 4) which contain the hyperfine-shifted protons originating from the cluster ligands. Starting with 4Fe Fd_B^{red}, which is purified under anaerobic and reducing conditions, oxidation of the cluster by O_2 can be detected by the rapid loss of peaks B_i^{red} (Figure 4A). Concomitantly, a spectrum (Figure 4B) appears which is similar, but not identical, to that of the final oxidation product, 4Fe Fd_A^{ox} (Figure 2B). The new spectrum (Figure 4B) exhibits four hyperfine-shifted and rapidly relaxing resonances in the range 10−15 ppm (Table 2); this new species is designated 4Fe Fd_B^{ox}. The temperature dependence of these peaks, labeled B_i^{ox}, is shown in Figure 3B, and chemical shifts for the aromatic side chains, as well as Val^{24} and Asn^{47}, are included in Table 1. When excess O_2 is incubated with the protein, the peaks of 4Fe Fd_B^{ox} slowly lose intensity[3] and a new set of peaks, A_i^{ox}, appear (Figure 4C). These resonances have the same chemical shifts, temperature dependence, and relaxation rates as those initially observed for fully oxidized 4Fe Fd_A^{ox}. With time, the 4Fe Fd_B^{ox} spectrum (Figure 4C) fully converts to the 4Fe Fd_A^{ox} spectrum (Figure 4D).

The addition of sodium dithionite to an Ar-purged sample of 4Fe Fd_A^{ox} immediately leads to a fourth set of hyperfine-shifted resonances, peaks A_i^{red} (Figure 4E), derived from the new species designated 4Fe Fd_A^{red}. These peaks A_i^{red} resonate in a spectral window indicative of a reduced cluster, but distinct from that of the anaerobically isolated reduced protein, 4Fe Fd_B^{red} (compare panels E and A in Figure 4). The temperature dependence of the six well-resolved low-field peaks A_i^{red} is shown in Figure 3D and the chemical shifts are listed in Table 2. In the presence of excess dithionite, and with time,[4] the peaks A_i^{red} lose intensity and the peaks B_i^{red} for 4Fe Fd_B^{red}, the anaerobically isolated form, reappear, thus closing the redox cycle. Eventually pure 4Fe Fd_B^{red} is formed and the cycle can be repeated. There was

[3] At 30 °C and pH 8.0, the rate of conversion from *Pf* 4Fe Fd_B^{ox} to 4Fe Fd_A^{ox} is dependent upon the O_2 concentration with approximate $t_{1/2}$ values of 83 h for air and 11 h for O_2.

[4] At 30 °C, pH 8.0, and 50 mM Tris, conversion from *Pf* 4Fe Fd_A^{red} to 4Fe Fd_B^{red} typically occurred with a $t_{1/2}$ of 10 h under conditions of excess dithionite.

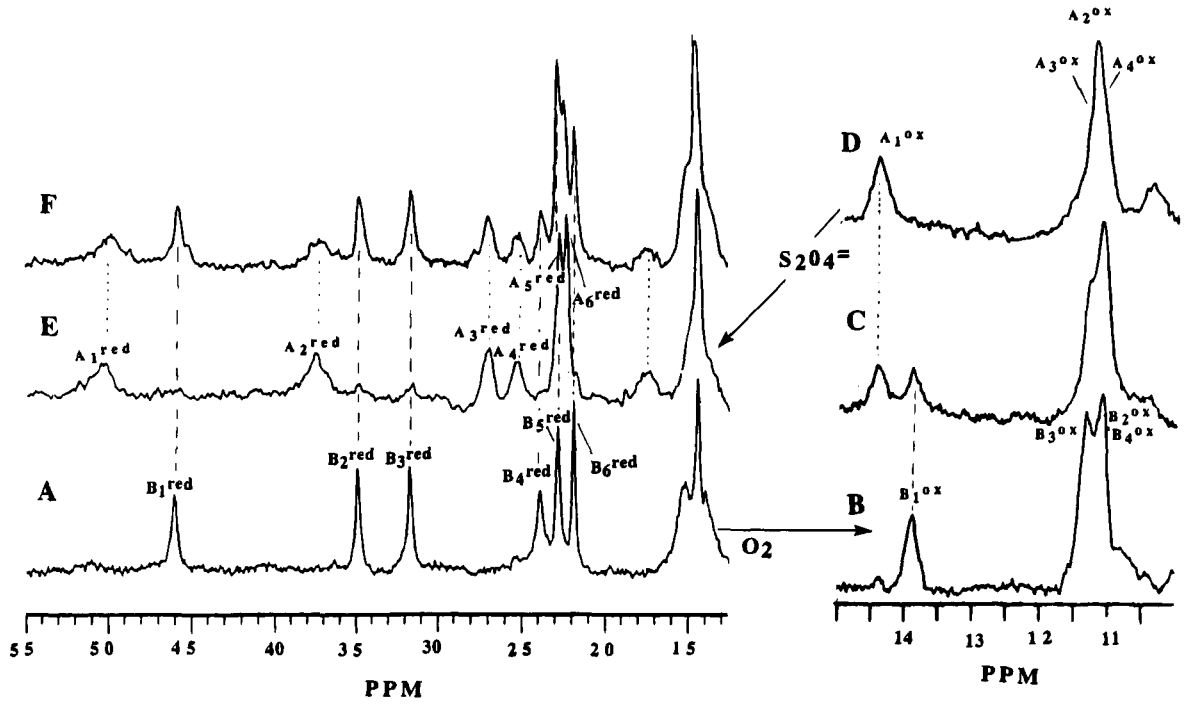

FIGURE 4: Resolved portions (to the low field of 10 ppm) of the 500-MHz ^{1}H NMR spectra of *Pf* 4Fe Fd where the contact-shifted and relaxed ligand signals resonate, as a function of the presence of oxidant (O_2), reductant ($S_2O_4^{2-}$), and time. (A) As-isolated *Pf* 4Fe Fd_B^{red}, with peaks B_i^{red}; (B) species formed immediately upon exposing 4Fe Fd_B^{red} to air at 30 °C, pH 8.0, designated *Pf* 4Fe Fd_B^{ox}, with peaks labeled B_i^{ox}; (C) the same sample as in panel B after 1 week open to the atmosphere at 30 °C, pH 8.0 (note loss of peaks B^{ox} and the appearance of new peaks we label A_i^{ox}); (D) the same sample as in panel B 5 weeks after opening to the atmosphere at 30 °C, pH 8.0, when now only a single species is present, designated *Pf* 4Fe Fd_A^{ox}, with peaks A_i^{ox}. (E) Addition of excess $S_2O_4^{2-}$ to the sample in panel D leads to appearance of a new species we designate *Pf* 4Fe Fd_A^{red}, with peaks A_i^{red}. (F) After 16 h at 30 °C, pH 8.0, and in the presence of excess $S_2O_4^{2-}$, peaks A_i^{red} lose intensity and are replaced by the characteristic peak B_i^{red} of the starting material *Pf* 4Fe Fd_B^{red} (whose spectrum in pure form is shown in trace A).

Table 2: Chemical Shifts for Hyperfine-Shifted Signals for *Pf* Fd[a]

	4Fe				3Fe[b]	
i in Q_i[c]	Fd_B^{red}	Fd_A^{red}	Fd_B^{ox}	Fd_A^{ox}	Fd_A^{ox}	Fd_B^{ox}
1	45.8	50.2	13.8	14.33	23.65	23.34
2	34.7	37.4	11.3	11.13	19.73	20.20
3	31.6	27.0	11.1	11.12	17.14	17.45
4	23.8	25.3	11.1	11.10	14.27	13.70
5	22.7	22.8			11.82	11.70
6	21.8	22.4			9.37	9.76

[a] Chemical shifts in parts per million from DSS, at 30 °C in ^1H_2O, pH 8.0. [b] Data for Fd_A^{ox} taken from Busse et al. (1992). [c] Peaks as labeled in Figures 4 and 6, with Q = A, B, a, b.

no evidence of protein degradation upon completing a cycle unless a large excess of O_2 is added, whereupon some 3Fe Fd and other degradation products are formed (Conover et al., 1990). Thus, four distinct forms of the *Pf* 4Fe Fd in the redox cycle, 4Fe Fd_A^{ox}, 4Fe Fd_B^{ox}, 4Fe Fd_A^{red}, and 4Fe Fd_B^{red}, can be identified, in which 4Fe Fd_B^{ox} and 4Fe Fd_A^{red} are metastable intermediates in the presence of excess oxidant and reductant, respectively. The redox origin of the A and B forms was elucidated as described below.

When 4Fe Fd_B^{red} is oxidized by limited O_2 followed by immediate deoxygenation, the conversion 4Fe Fd_B^{ox} to 4Fe Fd_A^{ox} is arrested, with less than 10% conversion over a 30-day (720-h) period. However, an identical sample that was left open to the atmosphere shows complete conversion to 4Fe Fd_A^{ox} over a much shorter time (data not shown; see supporting information). Moreover, when the deoxygenated sample, which had exhibited insignificant conversion to 4Fe Fd_A^{ox} over the 30-day period under anaerobic conditions, had O_2 bubbled through it, the conversion to 4Fe Fd_A^{ox} was complete within a day. Therefore, the conversion Fd_B^{ox} to Fd_A^{ox} is a slow, O_2-dependent reaction. Furthermore, preliminary results indicated that the conversion rate for 4Fe Fd_A^{red} to 4Fe Fd_B^{red} was dependent upon the reductant concentration.[5] The addition of various concentrations of sodium dithionite to 4Fe Fd_A^{ox} led to immediate reduction of the cluster, followed by a much slower and concentration-dependent conversion of the A to the B form (the lifetime was ~3 days for a sample of Fd_A^{red} in the presence of excess dithionite). The implication clearly is that the conversion of A to B is a slow, dithionite-dependent process. As might be expected, the initial studies showed that the rate of conversions of 4Fe Fd_B^{ox} to 4Fe Fd_A^{ox} and 4Fe Fd_A^{red} to 4Fe Fd_B^{red} in the presence of oxidant and reductant, respectively, is strongly accelerated at elevated temperature.[6]

Thiol Titration. The clear implication from the NMR data is that *Pf* Fd contains two types of redox centers, one of which is the 4Fe cluster. To investigate whether thiol/disulfide interconversion was responsible for the second redox site, the number of free thiols in the protein under the conditions of the NMR experiments was determined using DTNB. The four postulated redox states were prepared starting with the fully reduced (by sodium dithionite), anaerobically isolated 4Fe Fd. The dithionite was removed

[5] Sample reduction results in by-products of dithionite oxidation which themselves are oxidizing species. It is difficult, therefore, to interpret long-term reaction rates. Analyses of initial reaction kinetics, however, indicate a differential rate of conversion from Fd_A^{red} to Fd_B^{red} as a function of reductant concentration.

[6] Rates of conversion under conditions of excess oxidant or reductant were increased at elevated temperatures with $t_{1/2}$ values of 4 and 1.5 h at 70 °C for the conversion of Fd_B^{ox} to Fd_A^{ox} and Fd_A^{red} to Fd_B^{red}, respectively. Detailed studies of the temperature effects on rates are in progress.

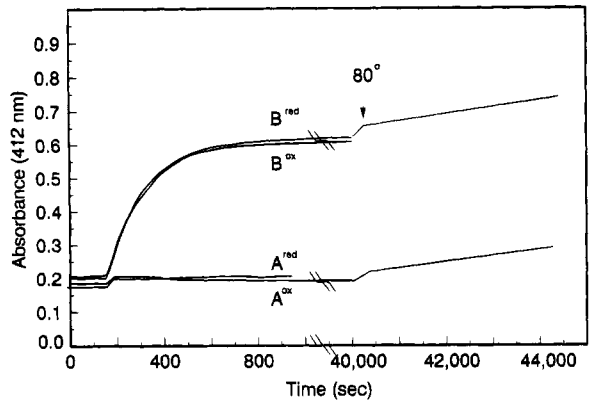

FIGURE 5: 4Fe Fd in each of the four redox states was incubated with 0.1 mM DTNB in pH 7.1, 0.1 M sodium phosphate buffer at 30 °C. The absorbance change at 412 nm was monitored. For A^{ox} and B^{red} the incubation temperature was changed to 80 °C after 16 h.

by gel filtration, and the four redox states were generated using stringent anaerobic techniques and controlled introduction of O_2 and degassing. The oxidation state of the cluster was determined by visible, EPR, and NMR spectroscopy. The results of the titration are shown in Figure 5. The reaction was complete within 5 min with no further change even after 12 h. Any cluster destruction would release 12 equiv of thiol and would be readily noted. Raising the temperature to 80 °C had minimal effect on the exposure of the cluster to DTNB reaction, which testifies to the stability of the molecule even after any free thiols have been reacted with DTNB. Both 4Fe Fd_B^{red} and 4Fe Fd_B^{ox} had 1.90 ± 0.05 free thiols/mol of protein, whereas 4Fe Fd_A^{red} and 4Fe Fd_A^{ox} had less than 0.1 thiol/mol of protein. These results are consistent with the A form containing the disulfide and the B form having two free thiols. When samples of 4Fe Fd_A^{ox} and 4Fe Fd_B^{ox} were each treated with excess sodium dithionite and then rapidly frozen in EPR tubes, both gave rise to spectra from a reduced 4Fe center, indicating rapid and quantitative reduction of the oxidized 4Fe centers in both forms of the protein. EPR spectra of 4Fe Fd_A^{red} and 4Fe Fd_B^{red} were indistinguishable (data not shown).

Conversion of 4Fe to 3Fe Fd. The ^1H NMR spectrum upon oxidation and partial (~20%) conversion of 4Fe Fd_B^{red} to the 3Fe Fd, by the addition of potassium ferricyanide under anaerobic conditions, yielded a sample with the ^1H NMR spectrum shown in Figure 6A. Five resolved nonlabile proton resonances, labeled b_i^{ox}, were identified with hyperfine shifts and temperature dependence very similar to, but clearly distinct from, those of the previously characterized 3Fe Fd^{ox} (Figure 6C, Teng et al., 1994; Gorst et al., 1994). The EPR spectrum of the sample exhibited g values for 3Fe Fd_B^{ox} the same as those reported for 3Fe Fd_A^{ox} (data not shown). The remaining 4Fe Fd_B^{ox} peaks are again labeled B_i^{ox}. Further anaerobic reaction with ferricyanide led to the loss of all signals B_i^{ox}, characteristic of 4Fe Fd_B^{ox} protein, and the appearance of signals of comparable intensity for 3Fe Fd_B^{ox} (peaks b_i^{ox}) and the previously characterized 3Fe Fd, which

[7] We note that the species B generally exhibits narrower resonances than the A species in both the reduced 4Fe Fd and the oxidized 3Fe Fd. For the latter protein, they are shown to arise from the dynamic averaging of alternate environments to Cys I and Cys IV, and a similar origin is assumed for the effect on reduced 4Fe Fd (Busse et al., 1992). The dynamic conformational heterogeneity near the cluster, therefore, appears to be a property of the protein where Cys 21 and Cys 48 form a disulfide bridge.

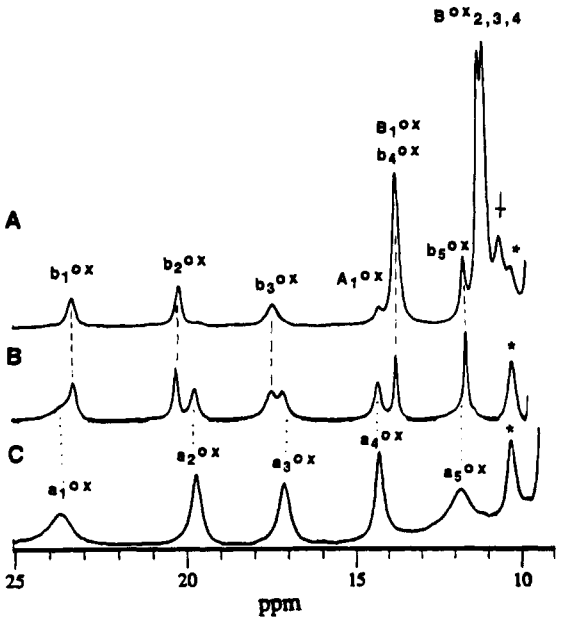

FIGURE 6: Resolved portions (to the low field of 10 ppm) of the 500-MHz ^1H NMR spectra in ^1H_2O, pH 8.0, at 30 °C of (A) the species resulting from anaerobically reacting 4Fe Fd_B^{red} with limited (~0.2 molar equiv) ferricyanide, which are identified as ~80% 4Fe Fd_B^{ox} with peaks B_i^{ox} and ~20% 3Fe Fd_B^{ox} with peak b_i; ~2% 4Fe Fd_A^{ox} is also observable with peaks A_i^{ox}. (B) Anaerobic reaction with excess ferricyanide leads to complete conversion to 3Fe Fd, with ~50% corresponding to the same species, 3Fe Fd_B^{ox} with peaks b_i^{ox}, initially generated in panel A above, and ~50% corresponding to the previously characterized 3Fe Fd^{ox} we designate as 3Fe Fd_A^{ox}, with peaks a_i^{ox} (Busse et al., 1992). (C) Aerobic reaction of 4Fe Fd_B^{red} with excess ferricyanide or incubation of 3Fe Fd_B^{ox} with O_2 results in complete formation of the previously characterized 3Fe Fd_A^{ox}, with peaks a_i^{ox}.

we designate as 3Fe Fd_A^{ox}, with peaks a_i^{ox}. In the absence of O_2, the ratio of 3Fe Fd_B^{ox} to 3Fe Fd_A^{ox} in Figure 6B was not significantly altered over 2 months (data not shown). However, upon introduction of O_2, the conversion to 3Fe Fd_A^{ox} was complete within a day, as shown by the spectrum in Figure 6C. The spectrum of 3Fe Fd_A^{ox} is identical to that for the equilibrium oxidized protein reported previously (Busse et al., 1992; Teng et al., 1994; Gorst et al., 1994). When reaction of 4Fe Fd_B^{red} with ferricyanide to form 3Fe Fd is carried out aerobically, only the 3Fe Fd_A^{ox} is isolated. Hence, it is clear that the conversion of $3Fd_B^{ox}$ to $3Fe_A^{ox}$ is an oxidation reaction. The chemical shifts for the hyperfine-shifted Cys resonances for 3Fe Fd_A^{ox} and 3Fe Fd_B^{ox} are included in Table 2.

Reactivity Properties of the A and B Form of Fd. A sample of 4Fe Fd_B^{red} was allowed to oxidize in air until it contained comparable amounts of 4Fe Fd_A^{ox} and 4Fe Fd_B^{ox}, as reflected by the 1:1 intensity ratio in peak A_1^{ox} and B_1^{ox}, and was degassed with Ar. Addition of 0.3 molar equiv of dithionite/total Fd^{ox} instantaneously led to loss in intensity for peaks A_1^{ox} and B_1^{ox} and generation of comparable intensity for peak A_1^{red} and B_1^{red} for the newly generated 4Fe Fd_A^{red} and 4Fe Fd_B^{red} respectively (not shown; see supporting information).

The sample of ~80% 4Fe Fd_B^{ox} and ~20% 3Fe Fd_B^{ox}, generated by partial reaction of 4Fe Fd_B^{red} with ferricyanide (with ^1H NMR spectra as shown in Figure 6A), was exposed to air at 85 °C. The conversion of 4Fe Fd_B^{ox} to 4Fe Fd_A^{ox} versus that of 3Fe Fd_B^{ox} to 3Fe Fd_A^{ox} were followed by monitoring the relative peak intensities of B_1^{ox}, A_1^{ox}, b_2^{ox}, and a_2^{ox}, the optimally resolved peaks for the four relevant

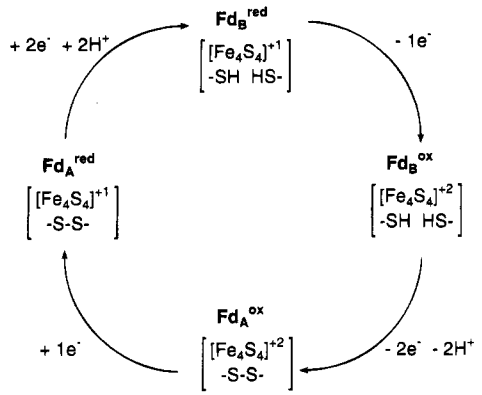

FIGURE 7: Proposed cycle for the four redox states of *Pf* Fd.

species (not shown; see supporting information). The ratios of peaks B_1^{ox}/A_1^{ox} and b_2^{ox}/a_2^{ox} were found to be inconsequentially altered in the course of the complete conversion to 4Fe Fd_A^{ox} and 3Fe Fd_A^{ox}.

Biological Function of the A and B Forms of Fd. Fd serves as an electron acceptor for several oxidoreductases during the fermentative metabolism of *Pf* (Adams, 1993) and excess reductant is disposed of both as H_2 and by the reduction of elemental sulfur (S^0) to H_2S. The A and B forms of *Pf* Fd were tested as electron carriers for pyruvate oxidation by *Pf* POR (Smith et al., 1994) and as electron donors to SuDH in a reconstituted system for H_2 production from pyruvate involving POR, SuDH, and hydrogenase (Ma et al., 1994). There was no detectable difference observed in the initial rate of H_2 production from such a system when either the A or B form was initially present in the assay mixture.

DISCUSSION

Identification of the Redox States for Pf 4Fe Fd. Four distinct states are observed by ^1H NMR spectroscopy in the redox cycle for *Pf* 4Fe Fd, and the chemical shift patterns and their temperature dependence for the individual forms, together with thiol titration data on the two forms with an oxidized cluster, dictate that the alternate "conformations" 4Fe Fd_A and 4Fe Fd_B are represented in Figure 1, panels A and B, respectively. Hence the complete redox cycle can be summarized as shown in Figure 7. The presence of a disulfide bond between Cys 21 and Cys 48 had been independently concluded on the basis of characteristic dipolar contacts in the NMR spectrum of 3Fe Fd_A^{ox} (Teng et al., 1994).

Interaction between Redox Centers. Both *Dg* 3Fe Fd and *Pf* 4Fe Fd can be cycled *in vitro* through four similar redox states involving the participation of both the cluster and disulfide bridge. For *Dg* 3Fe Fd, the metastable intermediates, analogous to the Fd_B^{ox} and Fd_A^{red} forms of *Pf* Fd, are only fractionally populated and at apparent kinetic equilibrium with Fd_A^{ox} and Fd_B^{red}, respectively (Macedo et al., 1994). This intrinsically will limit the degree to which any but the two "extreme" states of *Dg* 3Fe, Fd_A^{red} and Fd_B^{ox}, can be structurally characterized. For *Pf* 4Fe Fd, electron transfer involving the cluster is also rapid. This is evidenced by the observation of weak saturation-transfer between 4Fe Fd_B^{red} and 4Fe Fd_B^{ox}, as well as between 4Fe Fd_A^{red} and 4Fe Fd_A^{ox} (data not shown), and by the appearance/disappearance of the EPR signal of the $[4Fe-4S]^{1+}$ cluster when the oxidized/reduced protein is treated with excess dithionite/ferricyanide and then rapidly frozen for analysis. However, in contrast to *Dg* Fd, the electron/proton transfer and/or its subsequent conformational change in forming/breaking the disulfide bridge is extremely slow in *Pf* Fd at ambient temperature in the presence of either O_2 or dithionite. This spectroscopically advantageous property is presumably a result of the remarkable thermostability of this protein, which, when manipulated in its redox cycle well below its functional temperature, kinetically freezes out the two steps (by retarding the $2e^-/2H^+$ step) in the redox cycle. In other words, ambient temperature for this hyperthermophilic protein constitutes a form of "cryobiological" condition.

At this time it is not clear which of the four redox states presently identified in *Pf* 4Fe Fd are physiologically relevant *in vivo*. There was no noticeable difference in the ability of the A and B forms to function as an electron carrier for two *Pf* enzymes (POR and SuDH), although we have not investigated the redox state of the products when Fd (in the A or B form) is stoichiometrically reduced or oxidized by these enzymes. The chemical interconversion between the A and B forms in both cluster oxidation states is strongly accelerated at elevated temperatures, but at 80 °C, the minimum growth temperature of *Pf*, these processes still have a lifetime in excess of that needed for a viable reactive species in the presence of excess O_2 or excess dithionite. However, this A to B interconversion rate will be strongly dependent upon the chemical nature of the physiological oxidants and reductants. Obviously these are not O_2 and dithionite, which are, in fact, poor donors/acceptors for thiol redox chemistry. It is interesting to note the combination of the FeS cluster and a disulfide proved a potential mechanism for two facets of electron transfer during metabolic interconversions. First, Fd is a pathway by which one- and two-electron processes can converge or diverge. Second, Fd could serve as an interface between long-distance outer-sphere electron transfer (to and from the cluster) and inner-sphere electron transfer (via the disulfide). In this regard, Fd might have properties in common with flavoproteins.

It is noted that the ^1H NMR characterization of the 4Fe Fd from another hyperthermophile, *Thermococcus litoralis*, *Tl*, has shown that only two redox states are accessible with O_2 as oxidant and dithionite as reductant (Donaire et al., 1994). This Fd, like *Pf* and *Dg* Fd, possesses Cys^V and Cys^{VI} capable of forming a disulfide bridge. Preliminary 2D NMR data support the presence of this disulfide bridge in *Tl* 4Fe Fd^{ox}. The facile electron exchange between *Tl* 4Fe Fd^{ox} and 4Fe Fd^{red} indicates that the disulfide bridge is maintained in both redox states in solution at ambient temperatures. Hence the disulfide bridge is not as readily reduced in *Tl* 4Fe Fd as it is in *Pf* 4Fe Fd. The molecular structural properties that modulate the thermodynamics and kinetics of disulfide reduction in the various Fds are obscure at this time. Indeed, the 4Fe form of *Dg* Fd apparently lacks a disulfide bridge, in contrast to the 3Fe form (Macedo et al., 1994). The ^1H NMR molecular structures of the 4Fe Fds from both *Pf* and *Tl* are under investigation.

The essentially invariant ratio of 4Fe Fd_B^{red} to 4Fe Fd_B^{ox} and 4Fe Fd_A^{red} to 4Fe Fd_A^{ox} upon rapid partial reduction by dithionite of a kinetically trapped mixture of 4Fe Fd_A^{ox} and 4Fe Fd_B^{ox} indicate that the reduction potential of the cluster is independent of the redox state of Cys^{21} and Cys^{48}. The hyperfine shift patterns for the ligated residues differ slightly for the A and B forms in both cluster oxidation states, but

the local structural changes, likely to involve small changes in ligand orientation, have minimal effect on the cluster redox properties. In addition, the architecture of the cluster (whether 3Fe or 4Fe) does not greatly influence the rate of thiol oxidation by O_2 in *Pf* Fd, although this appears not to be the case in *Dg* Fd (Macedo et al., 1994). Hence, we conclude electron transfer between the redox centers at 30 °C is very slow and undetected. However, constraints on the interactions between the two centers may also be a consequence of the temperature, such that at 30 °C, a quasicryogenic state, electron transfer barriers are increased compared to the functional temperature (above 80 °C).

Influence of Redox State on Protein Structure. Although the elucidation of the detailed structures of the four states of *Pf* 4Fe Fd is beyond the scope of this paper, NOESY and TOCSY maps at a single mixing time each (350 and 60 ms, respectively) have been collected on 4Fe Fd_A^{ox}, 4Fe Fd_B^{ox}, and 4Fe Fd_B^{red}, and a preliminary analysis hints at widespread minor structural accommodation for either cluster or disulfide oxidative changes. The currently available data involve the readily assigned aromatic side chains and their important dipolar contacts. Chemical shifts for Trp^2 and Phe^{25} side chains and the complete Val^{24}, Tyr^{46}, and Asn^{47} are listed in Table 1. Strong NOESY cross peaks are observed between Phe^{25} and Val^{24} and between Trp^2 and Tyr^{46} in all cases. These two prominent pairs of side-chain interactions reflect the conserved hydrophobic core (Val^{24}, Phe^{25}) and the interaction between the large β-sheet that includes the two termini and the long α-helix near the C-terminus. As found in 3Fe Fd^{ox} (Teng et al., 1994), the Tyr^{46} ring exhibits NOESY cross peaks to only two backbone NHs, those for Tyr^{46} itself and the adjacent Asn^{47}, for which the whole residue is readily assigned (see Table 1).

The NOESY cross-peak patterns are qualitatively maintained in the four redox states, indicating that the overall folding topology is not seriously altered (not shown). The influence of 3Fe versus 4Fe Fd_A^{ox} is minor on the five characterized residues (see Table 1). Similarly small shift changes are observed upon change in cluster redox state (4Fe Fd_B^{red} versus 4Fe Fd_B^{ox}). It is noted, however, that the degeneracy of the three sets of Phe^{25} ring proton signals is raised partially in all 4Fe Fd states, and in 4Fe Fd_B^{red} this leads to resolution of all three signals, although the chemical shift changes for the ring are small (≤0.12 ppm among the 4Fe Fd forms). On the other hand, selective and significant shift changes dependent on the Cys^{21}, Cys^{48} redox state (4Fe Fd_A^{ox} versus 4Fe Fd_B^{ox}) are observed for (among others) two peptide NHs in contact with the Tyr^{46} ring. The NHs of both Tyr^{46} and Asp^{47} on the α-helix B exhibit ~0.2 ppm upfield and downfield bias, respectively, in the B (free Cys) relative to the A (disulfide) form (see Table 1). These residues are adjacent to Cys^{48} (VI) on the same helix, with Tyr^{46} on this helix reflecting an important tertiary contact with the Trp^2 on the N-terminal strand of the triple-stranded β-sheet. The selective shift changes are consistent with a local structural accommodation following cleavage of the disulfide bond. The Tyr^{46} and Asn^{47} NH shift changes upon breaking the disulfide bridge are indicative of stronger and weaker hydrogen bonding, respectively; however, α-helix B appears to be maintained [see Busse et al. (1992)]. Preliminary data indicate that detailed ^1H NMR characterization of the influence on structure of the cluster and Cys^{21} (V), Cys^{48} (VI) oxidation states is attainable, and detailed studies on the two extreme and stable redox states 4Fe Fd_A^{ox} and 4Fe Fd_B^{red} are in progress.

ACKNOWLEDGMENT

We are indebted to Dr. S. C. Busse and Dr. J. S. de Rop for experimental assistance.

SUPPORTING INFORMATION AVAILABLE

Three figures showing conversion of 4Fe Fd_B^{ox} to 4Fe Fd_A^{ox} with time (Figure 1S) and 500-MHz ^1H NMR spectra of a partially reduced sample of a mixture of 4Fe Fd_A^{ox} and 4Fe Fd_A^{red} (Figure 2S) and of the formation of Fd_A from Fd_B in both the 3Fe and 4Fe forms (Figure 3S) (4 pages). Ordering information is given on any current masthead page.

REFERENCES

Adams, M. W. W. (1993) *Annu. Rev. Microbiol. 47*, 627−658.
Adman, E. T., Sieker, L. C., & Jensen, L. H. (1976) *J. Biol. Chem. 251*, 3801−3806.
Aono, S., Bryant, F. O., & Adams, M. W. W. (1989) *J. Bacteriol. 171*, 3433−3439l.
Banci, L., Bertini, I., & Luchinat, C. (1990) *Struct. Bond. 72*, 113−135.
Beinert, H. (1990) *FASEB J. 4*, 2483−2494.
Bertini, I., Briganti, F., Luchinat, C., Scozzafava, A., & Sola, M. (1991) *J. Am. Chem. Soc. 113*, 1237−1245.
Bertini, I., Briganti, F., Luchinate, C., Messori, L., Mannanni, R., Scozzafava, A., & Vallini, G. (1992) *Eur. J. Biochem. 204*, 831−835.
Bryant, F. O., & Adams, M. W. W. (1989) *J. Biol. Chem. 264*, 5070−5079.
Busse, S. C., La Mar, G. N., Yu, L. P., Howard, J. B., Smith, E. T., Zhou, Z. H., & Adams, M. W. W. (1992) *Biochemistry 21*, 11952−11962.
Cammack, R., Dickson, D., & Johnson, C. (1977) in *Iron Sulfur Proteins* (Lovenberg, W., Ed.) Vol. III, pp 283−330, Academic Press, New York.
Conover, R. C., Kowal, A. T., Fu, W., Park, J.-B., Aono, S., Adams, M. W. W., & Johnson, M. K. (1990) *J. Biol. Chem. 265*, 8533−8541.
Donaire, A., Gorst, C. M., Zhou, Z.-H., Adams, M. W. W., & La Mar, G. N. (1994) *J. Am. Chem. Soc. 116*, 6841−6849.
Duee, E. D., Fanchon, E., Vicat., J., Sieker, L. C., Meyer, J., & Moulis, J. M. (1994) *J. Mol. Biol.* 243, 683−695.
Fukuyama, K., Nagahara, Y., Tsukihara, T., Katsube, Y., Hase, T., & Matsubara, H. (1988) *J. Mol. Biol. 199*, 183−193.
Gorst, C. M., Yeh, Y.-H., Teng, Q., Calzolai, L., Zhou, Z.-H., Adams, M. W. W., & La Mar, G. N. (1994) *Biochemistry* (in press).
Inubushi, T., & Becker, G. (1983) *J. Magn. Reson. 51*, 128−133.
Kissinger, C. R., Sieker, L. C., Adman, E. T., & Jensen, L. H. (1991) *J. Mol. Biol. 219*, 693−715.
Luchinat, C., & Ciurli, S. (1993) *Biol. Magn. Reson. 12*, 357−420
Ma, K., & Adams, M. W. W. (1994) *J. Bacteriol. 176*, 6509−6517.
Ma, K., Zhou, Z.-H., & Adams, M. W. W. (1994) *FEMS Microbiol. Lett. 122*, 263−266.
Macedo, A. L., Moura, I., Surerus, K. K., Papaefthymiou, V., Liu, M. Y., LeGall, J., & Münck, E. (1994) *J. Biol. Chem. 269*, 8052−8058.
Marion, D., & Guerlesquin, F. (1989) *Biochem. Biophys. Res. Commun. 159*, 592−598.
Park, J.-B., Fan, C., Hoffman, B., & Adams, M. W. W. (1991) *J. Biol. Chem. 266*, 19351−19356.
Phillips, W. D., & Poe, M. (1973) in *Iron Sulfur Protein* (Lovenberg, W., Ed.) Vol. II, pp 255−285, Academic Press, New York.
Riddles, P. W., Blakeley, R. L., & Zerner, B. (1983) *Methods Enzymol. 91*, 49−60.
Smith, E. T., Blamey, J. M., & Adams, M. W. W. (1994) *Biochemistry 33*, 1008−1016.
Teng, Q., Zhou, Z., Smith, E., Busse, S., Howard, J., Adams, M. W. W., & La Mar, G. N. (1994) *Biochemistry 33*, 6316−6326.

BI950359D